Available online at www.sciencedirect.com

ScienceDirect

IFAC PapersOnline CONFERENCE PAPER ARCHIVE

IFAC PapersOnLine 54-3 (2021) 158–163

A time-dependent model of pressure drop in reverse osmosis spiral wound membrane modules

A. Ruiz-García * **I. Nuez** *

* *Department of Electronic Engineering and Automation, University of Las Palmas de Gran Canaria, 35017 Spain (e-mail: alejandro.ruiz@ulpgc.es).*

Abstract: Reverse osmosis (RO) is the leading technology in desalination for both, brackish and seawater. Modeling RO process is a complex task as there are a high dependence on the operating conditions and feedwater characteristics. One of the main drawbacks of this technology is the performance decay due to fouling impact. Usually, fouling make the pressure drop to increase. This increase has not been reflected in the proposed models in RO process. The aim of this work was to proposed a time-dependent model for the pressure drop in RO process. For this purposes long-term experimental data of two full-scale brackish water RO desalination plants with two stages each were used. The first desalination plant was operating along 11 years in continuous regime while the second desalination plant was in operation during 14 years in intermittent regime. In the first desalination plant, the pressure drop ranges were 75-250 kPa and 25-150 kPa in the first and second stage respectively while in the second desalination plant were 50-200 kPa and 20-125 kPa. The behavior of the experimental data in both cases was close to an exponential function. The mentioned function was fitted in time domain using the standard deviation as error function.

Keywords: Process modeling and identification, time varying parameter plant, pressure drop, reverse osmosis, fouling.

1. INTRODUCTION

Reverse osmosis (RO) is the most widespread desalination technology for both seawater and brackish water. This has led to numerous attempts to improve its reliability and efficiency by using new materials Aani et al. (2018), optimizing the RO system design Ruiz-García and de la Nuez-Pestana (2018) and studying different feed spacer geometries (FSGs) Wang et al. (2019) with its impact on commercial spiral-wound elements Ruiz-García and de la Nuez Pestana (2019). Feed spacers geometry has a relevant impact,among other things, on pressure drop (Δp) in RO systems.

Usually, the effect of FSGs on Δp is shown through the friction factor (λ), which depend on Reynolds number (Re) and two parameters (a_1 and b_1) (1). The mentioned coefficient are determined by using computational fluid dynamics (CFD) and/or experimental procedures. The feed spacers has different characteristics such as material, filament cross-section, filament torsion, location of transverse filament, angle between crossing filaments (β), height of the feed channel (h), etc. A.H. Haidari et al. (2018b) that influence the RO process performance.

$$\lambda = a_1 \cdot Re^{b_1} \tag{1}$$

There are several works published about hydrodynamics and pressure drop dealing with spacer geometries. Belfort and Guter (1972) evaluated various commercial spacers for electrodialysis process. They analyzed the spacers in terms of porosity, dead flow area capability, drag coefficient ($C_\mathrm{d} \equiv \lambda$) and pressure drop proposing some optimal spacer screens. Equation (2) show the expression for the C_d, parameters a_2, b_2 and c were calculated for different FSGs. Belfort and Guter (1972) also carried out a hydrodynamic work related to desalination by electrodialysis process. They proposed a turbulent flow theory by using the relation of Blasius (3) in a channel. Sonin and M. S. Isaacson (1974) studied the hydrodynamic performance of an electrochemical system taking into account the channel geometry with spacers (eddy promoters) and flow conditions. They proposed the (4) for a Re between 300 and 2,000.

$$\lambda = \left(\frac{a_2}{Re^{b_2}}\right) + c \tag{2}$$

$$\lambda = 0.316 \cdot Re^{-0.25} \tag{3}$$

$$\lambda = 20 \cdot \left(\frac{h}{l}\right)^{0.6} \cdot Re^{-0.5} \tag{4}$$

where h is the is the height of the feed channel and l the cylinder spacing between successive spacers. Chiolle et al. (1978) proposed a mathematical model for two RO membrane separated by a spacer net to treat seawater. Equation (5) was used to calculate the Δp. It can be seen

10.1016/j.ifacol.2021.08.235

that the authors used the equation of a previous work Belfort and Guter (1972) with $a_2 = 310$, $b_2 = 1$ and $c = 0$.

$$\frac{\mathrm{d}p}{\mathrm{d}x} = \left(\frac{310}{Re}\right) \cdot \rho \cdot \frac{v^2}{h} \tag{5}$$

where ρ is the density and v the cross flow velocity. Kuroda et al. (1983) measured Δp in channels with non permeable walls obtaining the parameters indicated in (1) for Re between 50 and 700. Schock and Miquel (1987) tested the performance of RO SWMMs (Filmtec$^{\mathrm{TM}}$ FT30, Toray PEC 100..) considering experimental work in spacer-filled channels. The presence of feed spacer reduces the cross section area, this should be taken into account when velocity in s SWMM is calculated. Effective area (A_{eff}) was estimated by the mentioned authors by calculating the porosity (ε). Equation (6) was obtained for $100 < Re < 1,000$.

$$\lambda = 6.23 \cdot Re^{-0.3} \tag{6}$$

Avlonitis et al. (1991) carried an experimental work using the SWMM Filmtec$^{\mathrm{TM}}$ FT30 SW. The experimental considered a range of operating pressure and temperature, 0.77 mm as h, which is the same value use by G. Shock and A. Miquel Schock and Miquel (1987) for the FT30 SWMM. Avlonitis et al. (1991) deduced the (7) for λ in the feed channel. Other interesting work was done by Bouchard et al. (1994) on modeling ultrafiltration membranes. For estimating Δp they used the (8), which has been also used by other authors Alhseinat and Sheikholeslami (2012); Chen et al. (2004) in a RO process.

$$\lambda = 309 \cdot Re^{-0.83} \tag{7}$$

$$\Delta p(x,t) = \Delta p_0 - \frac{12 \cdot K_{\mathrm{spacer}} \cdot \eta}{h^2} \int_0^x v(\xi,t)\mathrm{d}\xi \tag{8}$$

where Δp_0 is the initial pressure drop, η is the water viscosity, ξ is a dummy integration variable and $K_{\mathrm{spacer}}(\geq 1)$ is a coefficient to consider the effect of the spacer in the pressure drop along the membrane feed channel. A.R. Da Costa et al. (1994) calculated C_{d} for different spacer filled channels for ultrafiltration. Three spacer groups were identified based on their hydrodynamic performance (a_1 and b_1 values). Values from 0.36 to 7.38 and from 0.16 to 0.40 were obtained for a_1 and b_1 respectively. This work was used by Abbas (2005) in a simulation and analysis of and industrial brackish water RO (BWRO) desalination plant. C.C. Zimmerer and Kottke (1996) studied the variation of λ with Re for different inclination angles and with a dimensionless wavelength value of 5.5. They concluded that with a proper choice of geometric parameters, the to basic flow types (channel flow and corkscrew flow) can be overlapped to a mixing flow. A review about SWMMs and feed spacers was carried out by Schwinge et al. (2004). They remarked that SWMM optimization require to take into consideration the pressure loss due to spacer characteristics. They mentioned that the use of CFD instead of cell experiment should be use for understanding the flow, shear and pressure loss in SWMMs and assisting in the design of novel spacers. Geraldes et al. (2005) modified the correlation of λ established by Shock and Schock and Miquel (1987) (6) by adding an additional factor (K_λ) to take into consideration pressure losses in the feed of the PVs and SWMM fittings. In their work, these correlations were used to simulate and optimize medium-sized seawater RO (SWRO) processes. C.P. Koutsou et al. (2007) presented a numerical and experimental study about the effect of FSGs in spacer-filled channels.

A comparison of pressure drop with different FSGs was carried out. One of the conclusions was that the pressure drop is very sensitive to the angle between axial filaments and the attack angle. Kavianipour et al. (2017) used CFD simulation for estimating λ for different feed spacers: ladder-type, triple, wavy, submerged and plain. The used (1) and showed that the configuration with less pressure drop was the plain and with the highest was the ladder-type. Z. Han et al. carried out a couple of works based on simulations using CFD in SWMMs Han et al. (2018a,b). They studied different geometries by fitting λ using (1) Han et al. (2018a). The second work was about studying the flow pattern considering different feed spacers (cavity, zig-zag and submerge). In this work, the above mentioned correlation for λ was also fitted. A.J. Karabelas et al. (2018) studied the effect of feed spacer compression on SWMM performance. A comprehensive method for performance assessment of particular feed spacer types was proposed. A.H. Haidari et al. (2018a) evaluated the performance of different FSGs using a particle image velocimetry to assess the velocity profiles. They established that the estimation of the obtained velocity maps were reasonable on the horizontal plane but, further experimental investigations would be required to quantify the effect of velocity in the vertical direction. Other interesting work was carried out by A.H. Haidari et al. (2019), in this work, the effect of feed spacer orientation on hydraulic conditions was studied. Assessment of pressure drop results considering different attack angles was done, higher pressure losses were observed with flow attack angle of 45° than 90°. The authors used a correlation similar to (1) to determine λ.

In general, the CFD studies are focused on improving the design of FSGs by studying little pieces of spacer-filled channels due to computational capacity and calculation time required. The models obtained by CFD are complex and would require a lot of time to be directly applied to an entire RO system. This is the reason why some authors have deduced simple correlations from CFD studies for estimating λ. Some works have considered fouling effects on pressure drop using CFD simulation and/or experimental work in small cells. Fouling effect on pressure drop in commercial SWMMs should be taken into account by considering experimental data of full-scale desalination plants operating under real conditions. A model for estimating the pressure drop considering the mentioned fouling effects on RO systems in long-term operation has not been proposed so far. The aim of this work was to propose a model for estimating the pressure drop in full-scale RO systems. This model took into consideration the fouling effect by establishing a time dependent λ. This consideration is due to the fact that throughout the operating time (t), the SWMMs usually get fouled, which causes λ to vary. This affects the flow patterns in the feed channel. Experimental data of two full-scale BWRO desalination

plants Ruiz-García et al. (2018); Ruiz-García and Ruiz-Saavedra (2015) were used to evaluate and fit the proposed model.

2. MATERIAL AND METHODS

2.1 Experimental data

Both full-scale BWRO desalination plants are located northwest of island of Gran Canaria (Canary Islands, Spain). These plants and most of its operating data have been described in detail in previous works Ruiz-García and Ruiz-Saavedra (2015); Ruiz-García and Nuez (2020). Fig. 1 show a general diagram of the BWRO desalination plants where the feedwater sources were groundwater wells and cartridge filters and antiscalant dosing were used in the pre-treatment stage. In the first plant, the RO system was equipped with 5 PVs. The configuration was 3:2 and the number of elements by PV was 6. The membrane element used was the BW30-400 Filmtec^{TM}, whose characteristics are available in the literature Abbas (2005). The feedwater flow (Q_f) was 25 m^3/h and Q_p was about 15 m^3 h^{-1}. It should be considered that pressure is usually measured at the inlet and outlet of the PVs.

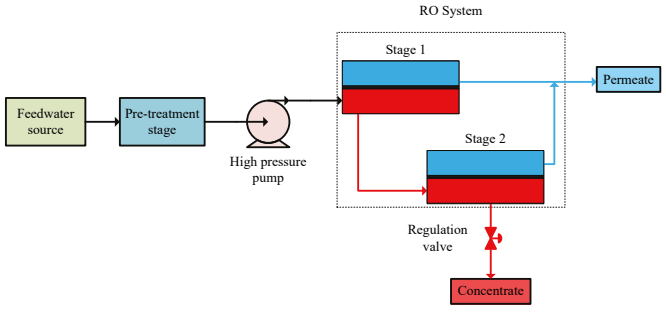

Fig. 1. Flow diagram of BWRO desalination plants.

The RO system of the second plant also had two stages but, 5 BWRO membrane elements per PV and element installed was the same as the in the first plant. The feed capacity of this BWRO desalination plant was around 17 m^3 h^{-1} and the production flow was between 10 and 11.5 m^3 h^{-1}. It should be considered that the operating data were measured in full-scale BWRO desalination plants where the dispersion of the experimental data are usual due to the operating conditions in such kind of plants (fluctuations, chemical cleaning in place, cartridge filters replacement, shut down and start-ups, etc.).

2.2 Pressure drop in spacer-filled channels

The modeling of pressure drop in the BWRO system was done considering some assumptions:

- Flat feed channels of the SWMMs.
- Only the pressure drop measured between the inlet and outlet the PV was considered.
- Constant feed-brine flow per stage (Q_{fb}).

Usually, when the flow regime is laminar the relation between shear stresses and velocity gradients is known. For unidirectional flow and non-compressible fluids, this relation is shown in (9).

$$\tau_{xy} = -\eta \cdot \frac{d\nu_x}{dy} \tag{9}$$

where τ_{xy} is the shear stress in the x direction, η is the water viscosity and ν_x the velocity in the x direction. In many cases, ν or pressure profiles are not easy to be calculated, particularly if the geometry is complicated as it happens in spacer-filled channels. In this cases, an average shear stress (τ_{av}) is used (10) Bird (2002).

$$\tau_{av} = \lambda \cdot \frac{\rho}{2} \cdot \nu_{av}^2 \tag{10}$$

where ρ is the water density and ν_{av} the average velocity. A momentum balanced applied in a flat feed channel gives (11):

$$\Delta p = \tau_{av} \cdot \frac{L \cdot P}{A} \tag{11}$$

where L is the feed channel length, P is the wetted perimeter and A is the cross section of the feed channel. The hydraulic diameter (d_h) is four times A divided by P. From (11) and (10), (12) is obtained. Considering that pressure is only x dependent and applying a momentum balance to an infinitesimal control volume in the feed spacer channel and changing the pressure order (13) is deduced. Equation (13) has been used previously in some works Geraldes et al. (2005); Du et al. (2014).

$$\Delta p = \lambda \cdot \frac{\rho}{d_h} \cdot \frac{\nu_{av}^2}{2} \cdot L \tag{12}$$

$$\frac{dp}{dx} = -\lambda \cdot \frac{\rho}{d_h} \cdot \frac{\nu_{av}^2}{2} \tag{13}$$

In this work, it was considered that pressure drop is operating time (t) dependent since when an RO system get fouled the pressure drop increases. Fouling in RO systems produce λ to change with the operating time, taking this into account, (1) could be written as (14).

$$\lambda = f(t) \cdot a_1 \cdot Re^{b_1} \tag{14}$$

where $f(t)$ is a function that depends on t. Equation (15) show the proposed expression for $f(t)$. Introducing (15) into (12), (16) was obtained. Usually, full-scale desalination plants work with constant permeate flow (Q_p). Constant feed-brine velocity (ν_{fb}) per stage was considered as in this sort of plants is not common to have measurement inside the PVs to check how ν_{fb} varies along the PVs (x direction) and with t. For determining the ν_{fb} per stage the software of the membrane manufacturer (WAVE) with the initial operating conditions was used. Concerning the first desalination plant, in the first stage a 77% of the Q_p was the estimated production and 23% in the second stage. 82% of the Q_p was the estimated production in the first stage and 18% in the second stage of the second desalination plant. After considering the pressure drop

depends on x and $\lambda(t)$, the variation of pressure drop with t can be written as (16). In this case x was constant as Δp_{fb} was measured between the beginning and the end of the PVs in both stages, x was assumed to be 6 m and 5 m respectively in both desalination plants.

$$f(t) = \delta \cdot \left(1 - \mathrm{e}^{-\frac{t}{T}}\right) \tag{15}$$

$$\Delta p(t) = \frac{\rho}{d_{\mathrm{h}}} \cdot \frac{\nu_{\mathrm{av}}^2}{2} \cdot x \cdot a_1 \cdot Re^{b_1} \cdot \delta \cdot \left(1 - \mathrm{e}^{-\frac{t}{T}}\right) \tag{16}$$

The index chosen in this paper is the standard deviation.

where $y_{\mathrm{i,exp}}$ are the experimental data, $y_{\mathrm{i,calc}}$ are the calculated data and N is the number of samples. The data collection frequency in the second plant was very variable. In the first 100 days of operation a high quantity of data were collected in comparison with the rest of the operating time. In order to avoid the fitting was centered where there are more experimental points (first 100 days) the Integral of Time multiplied by Squared Error ($ITSE$) was used, since we are interested in the behavior of the pressure drop in long-term.

3. RESULTS AND DISCUSSION

Figs. 2 and 3 shows the pressure drop of the first BWRO desalination plant in stage 1 and 2 respectively. Pressure drop in stage 1 was between 75 and 250 kPa while in the second stage was between 25 and 150 kPa. In the first stage, quite high values can be observed between the operation days 1,500 and 2,000. This was cause of high fouling effect on BWRO during that period that corresponded with a notable decrease in the water permeability coefficient Ruiz-García and Ruiz-Saavedra (2015). The high values in the second stage in the end of operating time were due scaling, mainly calcium carbonate Ruiz-García et al. (2018).

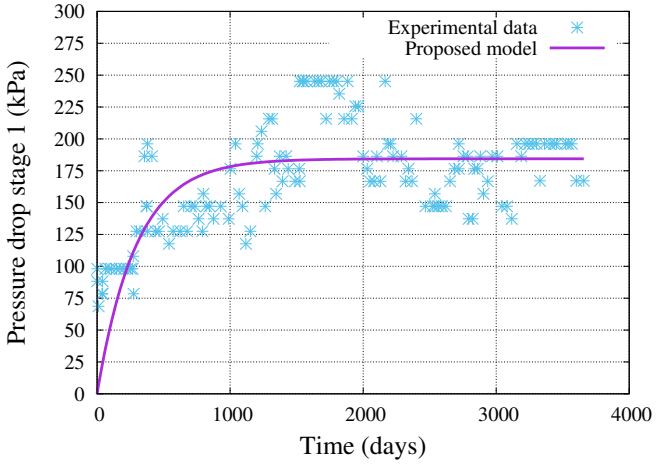

Fig. 2. Pressure drop in stage 1 in the first BWRO desalination plant.

In the second BWRO desalination plant, pressure drop in stage 1 was between 50 and 200 kPa while in the second stage was between 20 and 125 kPa as it can be seen in

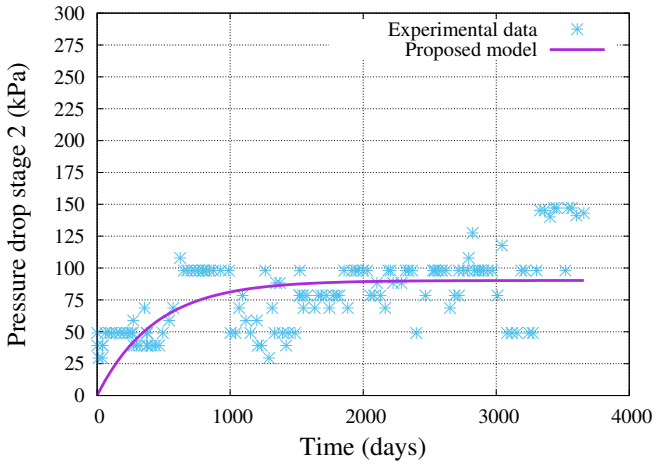

Fig. 3. Pressure drop in stage 2 in the first BWRO desalination plant.

Figs. 4 and 5. In general, the values were lower in comparison with the first desalination plant causes les BWRO membrane modules were disposed in series in each stage. It should be remarked that the first desalination plant was operating continuously while the second desalination plant operated intermittently. Beside this, more chemical cleanings were carried out in the first plant than in the second, these operating conditions affected the performance of both desalination plants in terms of fouling impact and it also affects the pressure drops in each stage throughout the operating time.

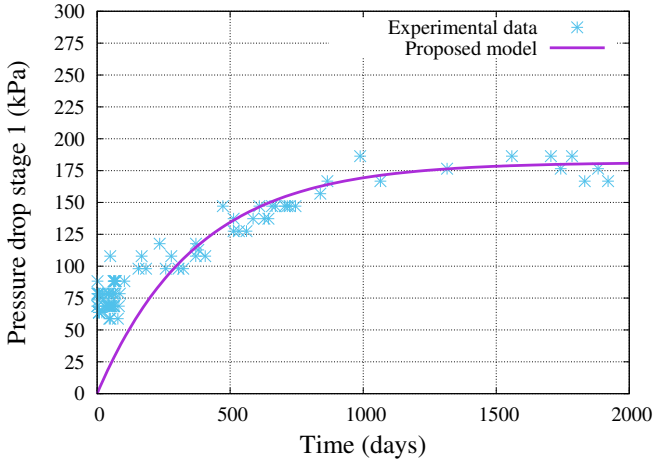

Fig. 4. Pressure drop in stage 1 in the second BWRO desalination plant.

Table 1 shows the values of the calculated parameters for the proposed model. The time constants (T) were quite different in the second plant from one stage to another. This was because the pressure drop in the second stage show a faster stabilization while in the first stage the pressure drop increased along the operating time. Probably, this was due to biofouling and colloidal fouling impact, which is usually higher in the first stage than in the second.

Table 1. Calculated parameters for each model

Parameter	Plant 1, stage 1	Plant 1, stage 2	Plant 2, stage 1	Plant 2, stage 2
δ	4.6898	3.0490	5.9381	2.7762
T	294.1176	434.7826	370.3704	166.6667
σ_{d} for plant 1, $ITSE$ for plant 2	2.8738	2.1473	1.5579×10^8	2.7617×10^8

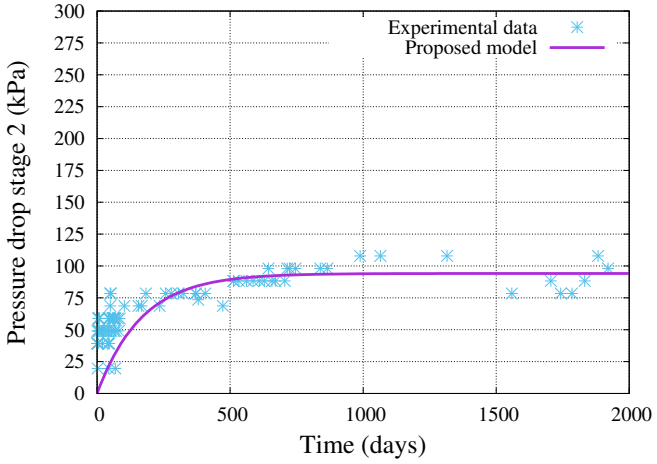

Fig. 5. Pressure drop in stage 2 in the second BWRO desalination plant.

4. CONCLUSIONS

A time-dependent model for the friction factor in filled channels of spiral wound membrane modules was proposed in this study. The experimental data showed a relatively fast increase at the beginning of the operating time and certain stabilization in long-term operation. This behavior resembles the proposed exponential function. Modeling RO process is complex as there are many variables that depends on the operating conditions and fluctuating water source characteristics, pressure drop is one of them that should be into consideration when control systems are designed for this sort of desalination plants.

REFERENCES

Aani, S.A., Haroutounian, A., Wright, C.J., and Hilal, N. (2018). Thin film nanocomposite (TFN) membranes modified with polydopamine coated metals/carbon-nanostructures for desalination applications. *Desalination*, 427, 60–74. doi:https://doi.org/10.1016/j.desal.2017.10.011. URL `http://www.sciencedirect.com/science/article/pii/S0011916417319793`.

Abbas, A. (2005). Simulation and analysis of an industrial water desalination plant. *Chem. Eng. Process.*, 44(9), 999–1004. doi:https://doi.org/10.1016/j.cep.2004.12.001. URL `http://www.sciencedirect.com/science/article/pii/S0255270105000097`.

A.H. Haidari, S.G.J. Heijman, and W.G.J. van der Meer (2018a). Effect of spacer configuration on hydraulic conditions using PIV. *Sep. Purif. Technol.*, 199, 9–19. doi:https://doi.org/10.1016/j.seppur.2018.01.022. URL `http://www.sciencedirect.com/science/article/pii/S1383586617336948`.

A.H. Haidari, S.G.J. Heijman, and W.G.J. van der Meer (2018b). Optimal design of spacers in reverse osmosis. *Sep. Purif. Technol.*, 192, 441–456. doi:https://doi.org/10.1016/j.seppur.2017.10.042. URL `http://www.sciencedirect.com/science/article/pii/S1383586617324188`.

A.H. Haidari, S.G.J. Heijman, W.S.J. Uijttewaal, and W.G.J. van der Meer (2019). Determining effects of spacer orientations on channel hydraulic conditions using PIV. *J. Water Process Eng.*, 31, 100820. doi:https://doi.org/10.1016/j.jwpe.2019.100820. URL `http://www.sciencedirect.com/science/article/pii/S2214714418303696`.

Alhseinat, E. and Sheikholeslami, R. (2012). A completely theoretical approach for assessing fouling propensity along a full-scale reverse osmosis process. *Desalination*, 301, 1–9. doi:https://doi.org/10.1016/j.desal.2011.12.014. URL `http://www.sciencedirect.com/science/article/pii/S0011916411010344`.

A.R. Da Costa, A.G. Fane, and D.E. Wiley (1994). Spacer characterization and pressure drop modelling in spacer-filled channels for ultrafiltration. *J. Membr. Sci.*, 87(1), 79–98. doi:https://doi.org/10.1016/0376-7388(93)E0076-P. URL `http://www.sciencedirect.com/science/article/pii/0376738893E0076P`.

Avlonitis, S., W.T. Hanbury, and Boudinar, M. (1991). Spiral wound modules performance. An analytical solution, part I. *Desalination*, 81(1), 191–208. doi:https://doi.org/10.1016/0011-9164(91)85053-W. URL `http://www.sciencedirect.com/science/article/pii/001191649185053W`. Proceedings of the Twelfth International Symposium on Desalination and Water Re-use.

Belfort, G. and Guter, G.A. (1972). An experimental study of electrodialysis hydrodynamics. *Desalination*, 10(3), 221–262. doi:https://doi.org/10.1016/S0011-9164(00)82001-9. URL `http://www.sciencedirect.com/science/article/pii/S0011916400820019`.

Bird, R.B. (2002). Transport phenomena . *Applied Mechanics Reviews*, 55(1), R1–R4. doi:10.1115/1.1424298. URL `https://doi.org/10.1115/1.1424298`.

Bouchard, C.R., Carreau, P.J., Matsuura, T., and Sourirajan, S. (1994). Modeling of ultrafiltration: Predictions of concentration polarization effects. *J. Membr. Sci.*, 97, 215–229. doi:https://doi.org/10.1016/0376-7388(94)00164-T. URL `http://www.sciencedirect.com/science/article/pii/037673889400164T`.

C.C. Zimmerer and Kottke, V. (1996). Effects of spacer geometry on pressure drop, mass transfer, mixing behavior, and residence time distribution. *Desalination*, 104(1), 129–134. doi:https://doi.org/10.1016/0011-9164(96)00035-5. URL `http://www.sciencedirect.com/science/article/pii/0011916496000355`.

Chen, K.L., Song, L., Ong, S.L., and Ng, W.J. (2004). The development of membrane fouling in full-scale RO processes. *J. Membr. Sci.*, 232(1), 63–72. doi:https://doi.org/10.1016/j.memsci.2003.11.028. URL `http://www.sciencedirect.com/science/`

article/pii/S0376738803006082.

Chiolle, A., Gianotti, G., Gramondo, M., and Parrini, G. (1978). Mathematical model of reverse osmosis in parallel-wall channels with turbulence promoting nets. *Desalination*, 26(1), 3–16. doi: https://doi.org/10.1016/S0011-9164(00)84124-7. URL http://www.sciencedirect.com/science/article/pii/S0011916400841247.

C.P. Koutsou, S.G. Yiantsios, and A.J. Karabelas (2007). Direct numerical simulation of flow in spacer-filled channels: Effect of spacer geometrical characteristics. *J. Membr. Sci.*, 291(1), 53–69. doi: https://doi.org/10.1016/j.memsci.2006.12.032. URL http://www.sciencedirect.com/science/article/pii/S0376738806008532.

Du, Y., Xie, L., Liu, J., Wang, Y., Xu, Y., and Wang, S. (2014). Multi-objective optimization of reverse osmosis networks by lexicographic optimization and augmented epsilon constraint method. *Desalination*, 333(1), 66–81. doi:https://doi.org/10.1016/j.desal.2013.10.028. URL http://www.sciencedirect.com/science/article/pii/S0011916413005109.

Geraldes, V., Pereira, N.E., and Norberta de Pinho, M. (2005). Simulation and Optimization of Medium-Sized Seawater Reverse Osmosis Processes with Spiral-Wound Modules. *Ind. Eng. Chem. Res.*, 44(6), 1897–1905. doi: 10.1021/ie049357s. URL https://doi.org/10.1021/ie049357s.

Han, Z., Terashima, M., Liu, B., and Yasui, H. (2018a). CFD investigation of the Effect of the Feed Spacer on Hydrodynamics in Spiral Wound Membrane Modules. *Mathematical and Computational Applications*, 23(4). doi:10.3390/mca23040080. URL https://www.mdpi.com/2297-8747/23/4/80.

Han, Z., Terashima, M., Liu, B., and Yasui, H. (2018b). Impact of Modified Spacer on Flow Pattern in Narrow Spacer-Filled Channels for Spiral-Wound Membrane Modules. *Environments*, 5(11). doi:10.3390/environments5110116. URL https://www.mdpi.com/2076-3298/5/11/116.

Karabelas, A.J., Koutsou, C.P., and Sioutopoulos, D.C. (2018). Comprehensive performance assessment of spacers in spiral-wound membrane modules accounting for compressibility effects. *J. Membr. Sci.*, 549, 602–615. doi:https://doi.org/10.1016/j.memsci.2017.12.037. URL http://www.sciencedirect.com/science/article/pii/S0376738817326121.

Kavianipour, O., Ingram, G.D., and Vuthaluru, H.B. (2017). Investigation into the effectiveness of feed spacer configurations for reverse osmosis membrane modules using Computational Fluid Dynamics. *J. Membr. Sci.*, 526, 156–171. doi:https://doi.org/10.1016/j.memsci.2016.12.034. URL http://www.sciencedirect.com/science/article/pii/S037673881631626X.

Kuroda, O., Takahashi, S., and Nomura, M. (1983). Characteristics of flow and mass transfer rate in an electrodialyzer compartment including spacer. *Desalination*, 46(1), 225–232. doi: https://doi.org/10.1016/0011-9164(83)87159-8. URL http://www.sciencedirect.com/science/article/pii/0011916483871598.

Ruiz-García, A., Melián-Martel, N., and Mena, V. (2018). Fouling characterization of RO membranes after 11years of operation in a brackish water desalination plant. *Desalination*, 430, 180–185. doi:https://doi.org/10.1016/j.desal.2017.12.046. URL http://www.sciencedirect.com/science/article/pii/S0011916417313164.

Ruiz-García, A. and Nuez, I. (2020). Long-term intermittent operation of a full-scale bwro desalination plant. *Desalination*, 489, 114526. doi: https://doi.org/10.1016/j.desal.2020.114526. URL http://www.sciencedirect.com/science/article/pii/S0011916420305403.

Ruiz-García, A. and Ruiz-Saavedra, E. (2015). 80,000h operational experience and performance analysis of a brackish water reverse osmosis desalination plant. Assessment of membrane replacement cost. *Desalination*, 375, 81–88. doi:https://doi.org/10.1016/j.desal.2015.07.022. URL http://www.sciencedirect.com/science/article/pii/S0011916415300308.

Ruiz-García, A. and de la Nuez-Pestana, I. (2018). A computational tool for designing BWRO systems with spiral wound modules. *Desalination*, 426, 69–77. doi:https://doi.org/10.1016/j.desal.2017.10.040. URL http://www.sciencedirect.com/science/article/pii/S0011916417310950.

Ruiz-García, A. and de la Nuez Pestana, I. (2019). Feed Spacer Geometries and Permeability Coefficients. Effect on the Performance in BWRO Spriral-Wound Membrane Modules. *Water*, 11(1), 1–13. doi:10.3390/w11010152. URL https://www.mdpi.com/2073-4441/11/1/152.

Schock, G. and Miquel, A. (1987). Mass transfer and pressure loss in spiral wound modules. *Desalination*, 64, 339–352. doi:https://doi.org/10.1016/0011-9164(87)90107-X. URL http://www.sciencedirect.com/science/article/pii/001191648790107X.

Schwinge, J., P.R. Neal, D.E. Wiley, D.F. Fletcher, and A.G. Fane (2004). Spiral wound modules and spacers: Review and analysis. *J. Membr. Sci.*, 242(1), 129–153. doi:https://doi.org/10.1016/j.memsci.2003.09.031. URL http://www.sciencedirect.com/science/article/pii/S0376738804003321. Membrane Engineering Special Issue.

Sonin, A.A. and M. S. Isaacson (1974). Optimization of Flow Design in Forced Flow Electrochemical Systems, with Special Application to Electrodialysis. *Ind. Eng. Chem. Proc. Des. Dev.*, 13(3), 241–248. doi:10.1021/i260051a009. URL https://doi.org/10.1021/i260051a009.

Wang, Y., He, W., and Müller, J.D. (2019). Sensitivity analysis and gradient-based optimisation of feed spacer shape in reverse osmosis membrane processes using discrete adjoint approach. *Desalination*, 449, 26–40. doi:https://doi.org/10.1016/j.desal.2018.09.016. URL http://www.sciencedirect.com/science/article/pii/S0011916418304132.